Doctoral Dissertation

Lysosomal acid lipase-regulating bioenergetic process is important for the cytodifferentiation of human periodontal ligament cells

ライソゾーム酸性リパーゼ誘導性エネルギー代謝制御によるヒト歯根膜細胞の分化制御機構の解明

Osaka University Graduate School of Dentistry

Course for Oral Science

(Department of Periodontology)

NANTAKEERATIPAT TEERACHATE

Supervised by

Professor Murakami Shinya

2023

This page is intentionally left blank.

Introduction

All cells require energy to maintain their physiological functions. Adenosine triphosphate (ATP), an organic molecule obtained upon the breakdown of energy substrates such as glucose, fatty acids (FAs), and amino acids, releases energy to fuel many cellular activities, including proliferation, inflammatory responses, and cytodifferentiation via multiple bioenergetic processes. For instance, increased ATP production is observed during the proliferation of fibroblasts, lipopolysaccharide (LPS)-induced inflammation via macrophage, and the cytodifferentiation of Th17 cells[1-4]. Similarly, osteoblasts require a large amount of ATP during their cytodifferentiation, and the total ATP production is increased for the synthesis of the matrix in calvarial pre-osteoblasts[5,6].

Typically, glucose is the primary energy substrate used to generate ATP and is transported to cells via the glucose transporter (GLUT) family. To generate ATP, glucose is converted to pyruvate for lactate-producing glycolysis and OXPHOS pathways[7]. OXPHOS can produce higher ATP levels compared to glycolysis. In addition to glucose, FAs and amino acids are used as energy sources for ATP production in the OXPHOS pathway as well[8]. FAs are primarily generated from the hydrolysis of lipids by lipases. Among

various lipases, a particular lipase functions depending on the types of lipids and their locations. For example, pancreatic lipase hydrolyzes dietary fats in the gut, and lipoprotein lipase hydrolyzes triglycerides (TGs) carried by lipoprotein molecules[9,10].

Lysosomal acid lipase (LAL) encoded by the lipase A (*LIPA*) gene functions in the lysosomes. It plays an important role in lipophagy, by hydrolyzing TGs and cholesteryl esters (CEs) in lipoproteins and lipid droplets (LDs) via the lysosomal-autophagic pathway to generate cholesterols and free FAs[11]. These molecules can be further used to generate ATP via FA oxidation followed by one of the major metabolic pathways, oxidative phosphorylation (OXPHOS)[12]. LAL is important for bone metabolism and mineralization. Helderman *et al*. showed that the cortical bone volume at the femur diaphysis and the osteoblast number are reduced in mice with LAL knockout and that the risk of bone fracture was higher in humans with LAL deficiency[13].

Periodontal ligament (PDL) is a unique connective tissue located between the cementum and alveolar bone and demonstrates various functions, such as stabilization of teeth in the alveolar bone, providing sensory input to the masticatory system, and distribution of appropriate force in the periodontal tissue[14]. Furthermore, it comprises heterogeneous cell populations and plays

an important role as a reservoir of mesenchymal stem cells that can differentiate into hard tissue-forming cells, such as osteoblasts and cementoblasts[15]. Energy metabolism is involved in PDL cytodifferentiation. For instance, enrichment analysis of PDL cells demonstrated OXPHOS as the highly upregulated pathway during cytodifferentiation[16]. In addition, high glucose (HG) and FA supplements influence the PDL cytodifferentiation[17-20]. Hence, the regulation of the energy metabolism during PDL cytodifferentiation might be a novel strategy for stimulating periodontal regeneration[21].

Previously, we identified a *LIPA* single nucleotide polymorphism (SNP), *LIPA* SNP rs143793106, as a risk variant of aggressive periodontitis (AgP) in the Japanese population[22]. This SNP causes a missense mutation of the amino acid position, resulting in the reduction of intracellular and extracellular LAL activity. However, it is still unknown how this SNP alters the protein structure of LAL. Interestingly, this SNP mediates the downregulation of calcification-related gene expression levels, calcified nodule formation, and alkaline phosphatase (ALPase) activity in human PDL (HPDL) cells with *LIPA* SNP during their cytodifferentiation[22]. Hence, it shows a negative influence on the cytodifferentiation of HPDL cells. However, the mechanisms underlying the suppression of the cytodifferentiation of HPDL cells mediated by *LIPA*/LAL are still not fully elucidated. We hypothesized

that *LIPA*/LAL induces the cytodifferentiation of PDL cells by regulating cellular energy metabolism as LAL is involved in FA-oxidation-dependent ATP production. In this study, we aimed to investigate the mechanism underlying the regulation of cytodifferentiation of HPDL cells mediated by LAL in terms of energy metabolism. We elucidated that LAL supports the cytodifferentiation of HPDL cells by mediating the adequate energy through the OXPHOS-related bioenergetic pathway.

Materials and methods

1. Reagents and cell lines

A specific LAL inhibitor, Lalistat-2, was purchased from Sigma-Aldrich (St. Louis, MO). HPDL cells were purchased from Lonza (BioWhittaker, Basel, Switzerland). HPDL cells were cultured and maintained in α-modified Eagle's medium (α-MEM) (Wako, Osaka, Japan) supplemented with 10% fetal bovine serum (FBS) (Thermo Fisher Scientific, Waltham, MA). For the osteogenic induction of HPDL cells, the cells were cultured in α-MEM supplemented with 10% FBS, 50 μg/mL of L-ascorbic acid (Wako), and 5 mmol/L of β-glycerophosphate (Sigma-Aldrich), as described previously[23].

2. Trypan blue exclusion

HPDL cells were cultured in 12-well plates ($1x10^5$ cells/well) with Lalistat-2 at different concentrations (0–100 μM). Cell viability was assessed by trypan blue exclusion, as described previously[24]. Briefly, the cell suspension was mixed with trypan blue reagent (Wako) in a 1:1 (vol/vol) ratio, and the numbers of viable and dead cells were counted using a Countess II Automated Cell Counter (Thermo Fisher Scientific).

3. Cell proliferation assay

Cell proliferation was analyzed using the bromodeoxyuridine (BrdU) incorporation assay. HPDL cells were seeded in 96-well plates ($1x10^4$ cells/well) and incubated with different concentrations of Lalistat-2 (0–100 μM). After 24 h of incubation, the BrdU incorporation assay was performed using a BrdU Cell Proliferation ELISA kit (Roche Applied Science, Mannheim, Germany) following the manufacturer's instructions. Briefly, cells were labeled using the BrdU labeling solution (10 μL/well) for 2 h. After removing the labeling solution, cell fixation was performed using FixDenat (200 μL/well) for 30 min. Then, the cells were treated with an anti-BrdU-POD working solution (100 μL/well) for 90 min at room temperature. After washing the cells using a wash buffer, they were incubated with a substrate solution for 15 minutes. After color development, the absorbance was measured at 450 nm to determine the BrdU incorporation ratio using a GloMax® 96 Microplate Luminometer (Promega, Madison, WI).

4. LAL and ALPase activity assay

LAL activity was determined using a LysoLive Lysosomal Acid Lipase Kit (Abcam, Cambridge, UK) according to the manufacturer's protocol. Briefly, HPDL cells were plated and incubated for 72 h. After washing the cells with 4 ºC phosphate-buffered saline (PBS) (Wako), 1 mL of α-MEM

containing 1 μL of *LIPA* substrate was added to the cells and incubated for 4 h. Finally, HPDL cells were collected and suspended with Flow Holding and Sorting Buffer (Abcam) and analyzed by CytoFLEX S Flow Cytometer (Beckman Coulter, Brea, CA). The ALPase activity assay was performed as described previously[25]. Briefly, after washing the cultured cells with PBS, 500 μL of Tris-HCl (pH 7.4) was added to the cells. The cells were sonicated for 30 s on ice using the Handy-Sonic model UR-20P (TOMY, Tokyo, Japan). After centrifuging the sonicated cells, the supernatant was collected and analyzed by a microplate reader (BioRad Laboratories, Hercules, CA).

5. Real-time PCR

Total RNA was extracted from HPDL cells cultured in 12-well plates ($1x10^5$ cells/well) using Maxwell RSC simply RNA Cells/Tissue Kit (Promega) and treated with DNase I (Takara Bio, Shiga, Japan). To synthesize cDNA, the isolated RNA was reverse transcribed using a High Capacity RNA-to-DNA kit (Applied Biosystems, Foster City, CA) according to the manufacturer's instructions. Real-time PCR was performed using StepOnePlus Real-time PCR System (Applied Biosystems) with Power PCR SYBR Master Mix (Applied Biosystems) and gene-specific PCR primers (Table 1) (Fasmac, Kanagawa, Japan, and Thermo Fisher Scientific). The expression level of each gene was calculated as a relative ratio to the

expression level of the hypoxanthine phosphoribosyltransferase-encoding gene (*HPRT*), which is an endogenous control gene.

Table 1. Gene-specific primers for real-time PCR

Gene	Primer sequence
Lipase A (*LIPA*)	F 5′-ACCTGGTCTGGAAACATAAGACAC-3′
	R 5′-TGCCTTGAGAATGACCCACATAA-3′
Alkaline Phosphatase	F 5'-GGACCATTCCCACGTCTTCAC-3'
(*ALPL*)	R 5'-CCTTGTAGCCAGGCCCATTG-3'
Collagen Type I Alpha 1	F 5'-CCCGGGTTTCAGAGACAACTTC-3'
Chain (*COL1A1*)	R 5'-TCCACATGCTTTATTCCAGCAATC-3'
Hypoxanthine	F 5'-GGCAGTATAATCCAAAGATGGTCAA-3'
Phosphoribosyltransferase	R 5'-GTCAAGGGCATATCCTACAACAAAC-3'
(*HPRT*)	
Runt-related Transcription	F 5′-CACTGGCGTGCAACAAGA- 3′
Factor 2	R 5′-CATTCCGGAGCTCAGCAGAATAA-3′
(*RUNX2*)	
Sp7 Transcription Factor	F 5′-GCCATTCTGGGCTTGGGTA- 3′
(*SP7*)	R 5′-TGTGGCAGGGCCAGAGTCTA-3′

Integrin Binding	F 5′-GGCCACGATATTATCTTTACAAGCA- 3′
Sialoprotein (*IBSP*)	R 5′-TCAGCCTCAGAGTCTTCATCTTCA-3′
ATP Synthase F1 Subunit	F 5′- ATGACGACTTATCCAAACAGGC- 3′
Alpha (*ATP5FA1*)	R 5′- CGGGAGTGTAGGTAGAACACAT-3′
Lactate Dehydrogenase A	F 5′- AGCCCGATTCCGTTACCT- 3′
(*LDHA*)	R 5′- CACCAGCAACATTCATTCCA-3′
Carnitine	F 5′- CCAGACGAAGAACGTGGTCA- 3′
Palmitoyltransferase 1A	R 5′- ATCTTGCCGTGCTCAGTGAA-3′
(*CPT1A*)	
Glucose Transporter 1	F 5′- CTGCTCATCAACCGCAAC- 3′
(*GLUT1*)	R 5′- CTTCTTCTCCCGCATCATCT-3′

F: Forward, R: Reverse

6. Alizarin red staining

Calcified nodule formation in HPDL cells in 12-well plates ($1x10^5$ cells/well) was analyzed using a modified alizarin red staining protocol as described previously[26]. Briefly, after removing the cell supernatant, the cell layer was washed with PBS and fixed with 100% cold ethanol (Wako) for 15 min. Then, the cell layer was washed with distilled water, stained with 1% Alizarin red S (pH 6.4) (Wako) for 5 min, and washed with distilled water. To quantify the amount of calcified nodules, the stained cell layer was scanned

with a scanner (EPSON GT-X970, EPSON, Nagano, Japan). ImageJ software (National Institute of Health, Bethesda, MD) was used for the analysis of the density of alizarin red-stained nodules.

7. Induction of LD and starvation

For LD induction, HPDL cells ($5x10^4$ cells) were cultured in a 35 mm dish and pre-loaded with 250 μM of oleic acid (OA) (adjusted from OA-albumin derived from bovine serum, Sigma-Aldrich) overnight. For starvation, OA-loaded HPDL cells were cultured in the α-MEM without FBS and co-treated with different concentrations of Lalistat-2 (0-100 μM) for 24 h.

8. Confocal microscopy

After osteogenic induction or starvation, the cells were fixed using 4% paraformaldehyde (Wako) and stained with 2 μM of BODIPY 493/503 (Thermo Fisher Scientific) and 1 μM of 4′,6-diamidino-2-phenylindole (DAPI) (Sigma-Aldrich). A Leica TCS SP8 confocal microscope (Leica Microsystems, Wetzlar, Germany) was used to visualize the nucleus and LDs in the cells. ImageJ software was used for the analysis of LDs.

9. Metabolic analysis

The metabolic phenotypes of HPDL cells were assessed using an XFp Extracellular Flux Analyzer (Seahorse Bioscience, North Billerica, MA) and machine-specific kits, including Seahorse XFp Real-Time ATP Rate Assay Kit (Agilent, Santa Clara, CA) and Seahorse XFp Cell Mito Stress Test Kit (Agilent). Briefly, cells were seeded in Seahorse XFp Cell Culture Miniplates (Agilent) ($8x10^4$ cells/well) and cultured in α-MEM supplemented with 10% FBS. One hour prior to the experiment, the medium was replaced with the assay medium (Seahorse XF DMEM Medium, pH 7.4 (Agilent) supplemented with 10 mM Seahorse XF Glucose (Agilent), 1 mM Seahorse XF Pyruvate (Agilent), and 2 mM Seahorse XF L-Glutamine (Agilent)). Then, the cells were incubated at 37 °C in a CO_2-free atmosphere. Real-Time ATP Rate Assay Kit and Cell Mito Stress Test Kit were utilized according to the manufacturer's instructions. For the Real-time ATP Rate Assay, basal oxygen consumption rate (OCR) and extracellular acidification rate (ECAR) were analyzed. Then, OCR and ECAR responses toward oligomycin (1.5 μM) and a combination of rotenone and antimycin (Rot/AA) (0.5 μM), which were administered via injections, were measured. For the Cell Mito Stress Test, OCR was analyzed. Next, OCR responses toward the application of oligomycin (1.5 μM), FCCP (2 μM), and Rot/AA (0.5 μM) were evaluated. Data were then analyzed using

online Agilent Seahorse Analytics (Agilent) and GraphPad Prism version 9.4.1 (San Diego, CA).

10. Statistical analysis

Student's t-test was used for comparing two groups, and one-way ANOVA was used for comparing three or more groups. The statistical significance was set at $p < 0.05$ for all statistical tests. Data were analyzed using GraphPad Prism version 9.4.1.

Results

1. Lalistat-2 inhibited LAL activity and LD utilization in HPDL cells

In this study, we used Lalistat-2, a LAL inhibitor, to analyze the involvement of LAL in the energy metabolism of HPDL cells during their cytodifferentiation with respect to mRNA expression, osteogenic phenotypes, and metabolic phenotypes, including LD utilization and bioenergetic profiles. To determine an appropriate concentration of Lalistat-2 in HPDL cells, we cultured HPDL cells with different concentrations of Lalistat-2 (0–100 μM). We then performed the LAL activity assay, the trypan blue exclusion, and the BrdU incorporation assay to analyze the effects of Lalistat-2 on the LAL activity, cell viability, and cell proliferation, respectively. We found that Lalistat-2 inhibited approximately 90% of LAL activity at concentrations of 10 and 100 μM concentration (Fig. 1A). However, it (0–100 μM) did not affect cell viability and proliferation (Fig. 1B and C). To analyze the effect of Lalistat-2 on LD utilization, we induced LD formation in HPDL cells using oleic acids (OA), then we treated the cells with Lalistat-2 (0–100 μM) in the absence of FBS, representing the starving condition in order to induce the LD utilization. We observed the formation of LDs in OA-loaded HPDL cells, indicating successful induction of LD formation (Fig. 1D). The OA-loaded HPDL cells cultured in the medium containing 10% FBS, the control group

representing the physiological condition. HPDL cells treated with or without 1 μM of Lalistat-2 showed significantly decreased LD counts compared to the control. In contrast, those treated with 10 and 100 μM of Lalistat-2 showed no significant differences in the remaining LDs, indicating that 10 and 100 μM of Lalistat-2 inhibited LD utilization in HPDL cells (Fig. 1D and E). Taken together, we found that 10 μM was the minimum concentration of Lalistat-2 that showed effectiveness in HPDL cells. To avoid the non-specific inhibitory effects on HPDL cells, we used 10 μM of Lalistat-2 in further experiments.

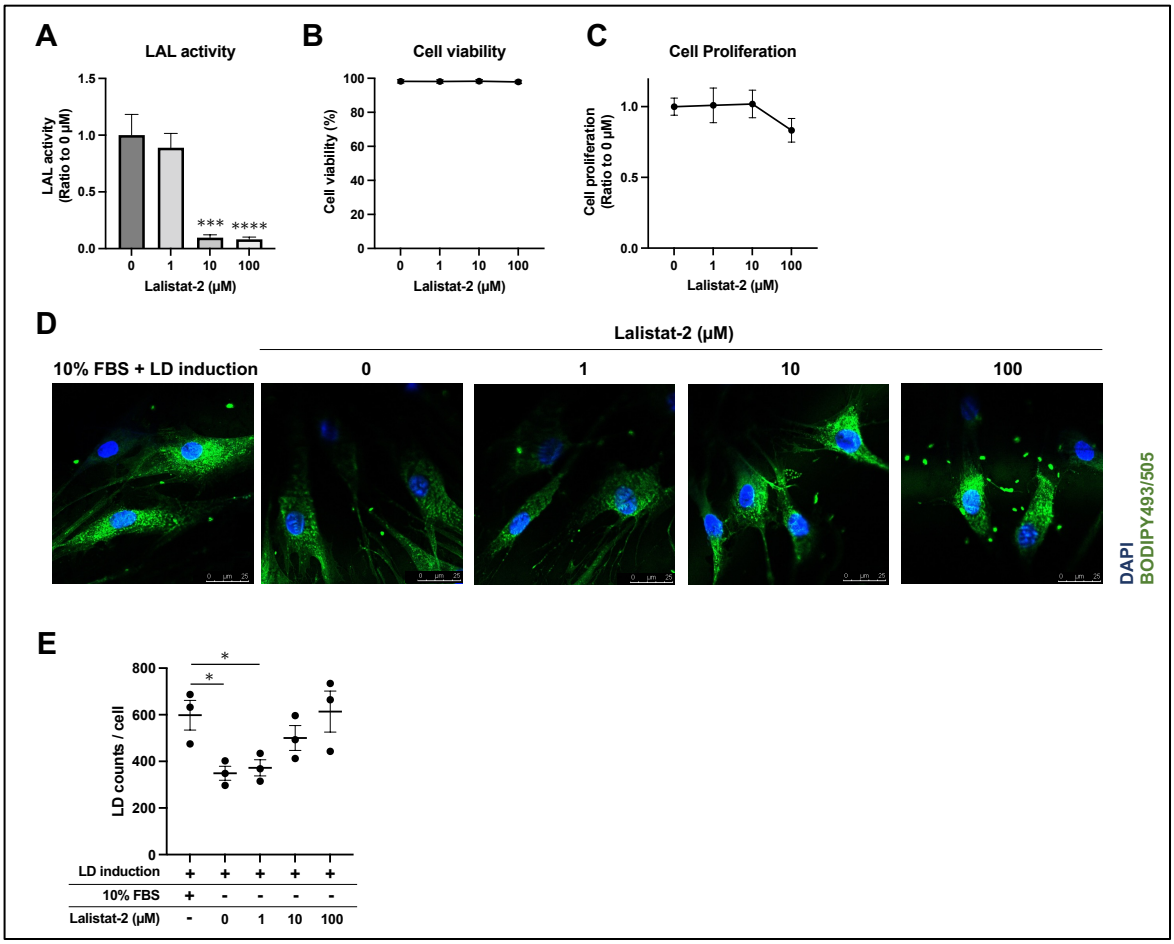

Fig. 1 Lalistat-2 inhibited LAL activity and LD utilization in HPDL cells.

HPDL cells were treated with Lalistat-2 (0–100 μM).

(A) LAL activity in HPDL cells was measured by the LAL activity assay. The graph shows the relative ratios of LAL activity obtained by normalizing it to that of untreated HPDL cells. ***$p<0.001$, ****$p<0.0001$ compared to 0 μM of Lalistat-2

(B) The cell viability was measured by the trypan blue exclusion assay.

(C) The cell proliferation was measured by the BrdU incorporation assay. The graph shows the relative ratios of the BrdU incorporation of HPDL cells treated with Lalistat-2 (0 - 100 μM) by normalizing to that of untreated HPDL cells.

(A-C) Data represent the average and standard deviation (SD) (n=3).

(D) Fluorescent staining was performed to detect LDs in HPDL cells using BODIPY493/505. The stained HPDL cells were imaged using a confocal microscope. Green: LDs (BODIPY493/505)

Blue: nuclei (4′,6-diamidino-2-phenylindole (DAPI)). Scale bar: 25 μm

(E) LD counts per cell in (D) were calculated by ImageJ. Data represent the average and SD (n=3). $^{*}p<0.05$ compared to the control (LD induction in the media with 10% FBS)

2. *LIPA*/LAL enhanced the cytodifferentiation of HPDL cells.

To confirm the involvement of *LIPA* in the cytodifferentiation of HPDL cells, we performed the osteogenic induction without or with Lalistat-2 treatment at a concentration of 10 μM. We then analyzed the mRNA expression levels of *LIPA* and calcification-related genes, including alkaline phosphatase (*ALPL*) and collagen type I alpha 1 chain (*COL1A1*) using real-time PCR. The mRNA expression of *LIPA* was up-regulated in a time-dependent manner as the expression of calcification-related genes was upregulated (Fig. 2). These results suggest the association of *LIPA* with the cytodifferentiation of HPDL cells. To further examine the involvement of LAL in the cytodifferentiation of HPDL cells, we performed the osteogenic induction of HPDL cells without or with Lalistat-2 treatment at a concentration of 10 μM. We then performed real-time PCR to assess the mRNA expression levels of calcification-related genes. Lalistat-2 significantly down-regulated mRNA expression of *ALPL*, *COL1A1,* and integrin-binding sialoprotein

(*IBSP*). In contrast, it showed no effect on the mRNA expression of runt-related transcription factor 2 (*RUNX2*) and Sp7 transcription factor (*SP7*) (Fig. 3A). We also performed the ALPase activity assay and alizarin red staining assay during the cytodifferentiation of HPDL cells. We found that Lalistat-2 significantly decreased ALPase activity and calcified nodule formation (Fig. 3B and C). These data indicate that LAL enhanced the cytodifferentiation and mineralization of HPDL cells.

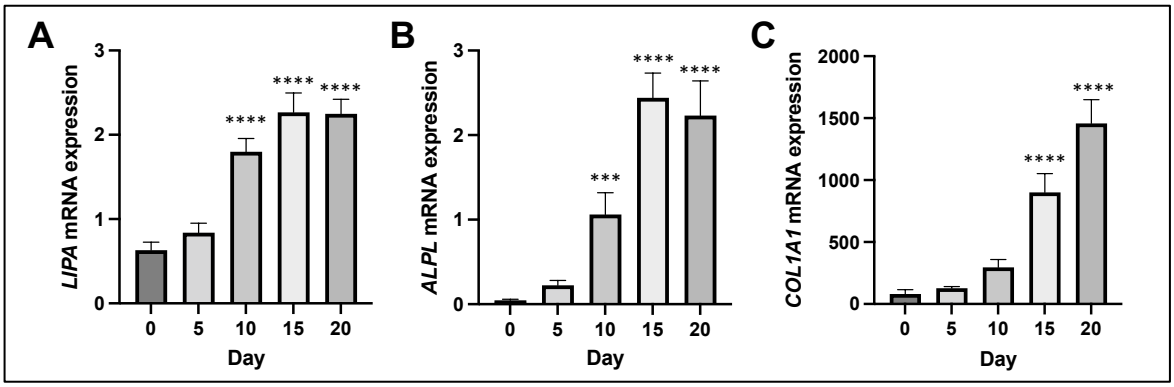

Fig. 2 *LIPA* mRNA expression was upregulated during the cytodifferentiation of HPDL cells.

HPDL cells were cultured in the osteogenic medium for 20 days. The mRNA expression levels of *LIPA* (*left*), *ALPL* (*middle*), and *COL1A1* (*right*) during the cytodifferentiation of HPDL cells were analyzed using real-time PCR. The expression of each gene was calculated as the relative ratio to that of HPRT (housekeeping control gene). Data represent the average and SD (n=4). $^{***}p<0.001$, $^{****}p<0.0001$ compared to day 0

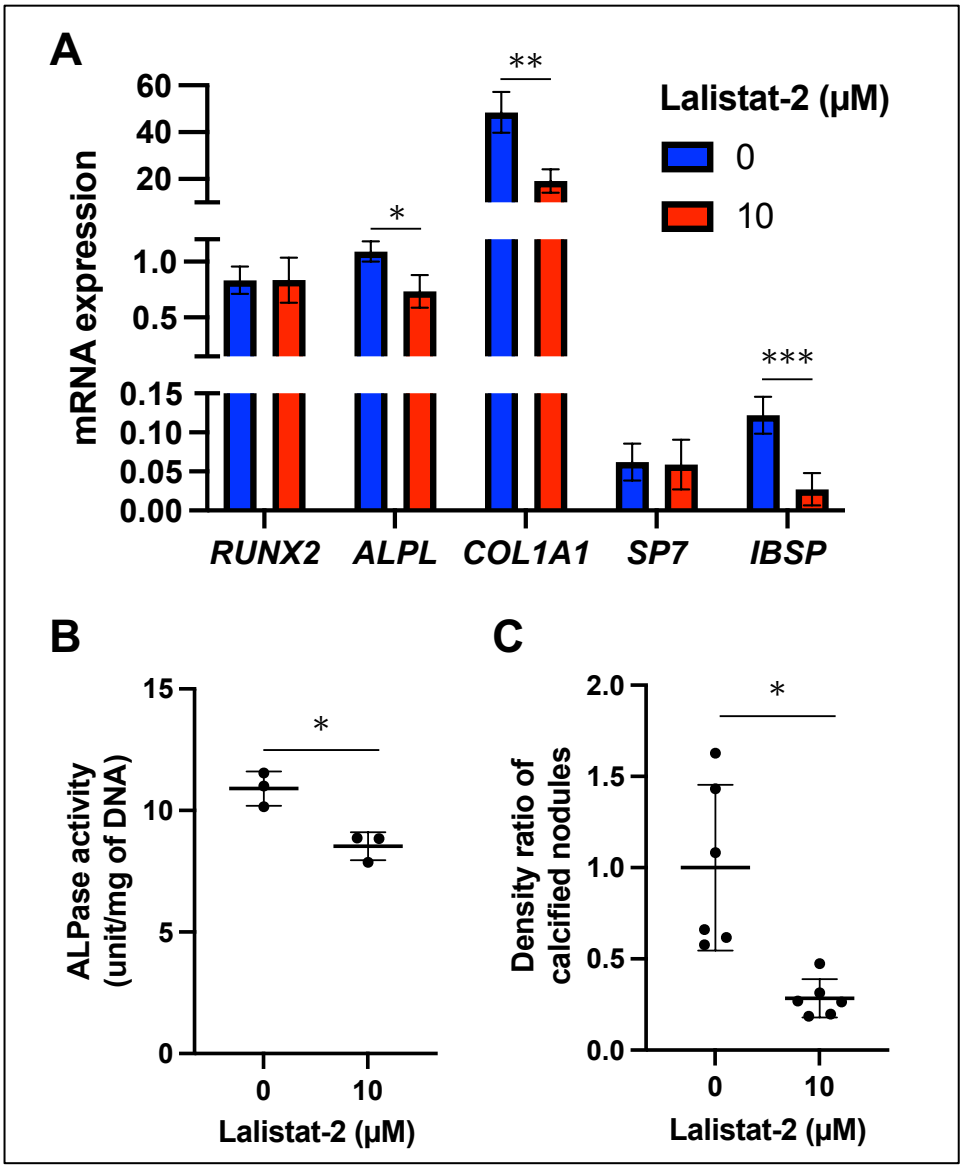

Fig. 3 Lalistat-2 suppressed the cytodifferentiation of HPDL cells.

HPDL cells were cultured in an osteogenic medium without or with Lalistat-2 at a concentration of 10 μM.

(A) The mRNA expression levels of *RUNX2*, *ALPL*, *COL1A1*, *SP7*, and *IBSP* on day 7 of the cytodifferentiation of HPDL cells were measured using real-time PCR. The expression of each gene was calculated as the relative ratio to that of *HPRT* (a housekeeping control gene). Data represent the average and SD (n=3).

(B) Alkaline phosphatase (ALPase) activity was measured on day 10 of cytodifferentiation of HPDL cells. Data represent the average and SD, and dots represent each individual (n=3).

(C) The calcified nodules were stained with alizarin red on day 21 of the cytodifferentiation of HPDL cells. The density of the calcified nodules was measured using ImageJ. The graph shows the relative ratio of the density of calcified nodules to that observed in the absence of Lalistat-2 (0 μM). Data represent the average and SD, and dots represent each individual (n=6).

$^{*}p<0.05$, $^{**}p<0.01$ compared to Lalistat-2 (0 μM)

3. LAL regulated OXPHOS-related genes during cytodifferentiation of HPDL cells.

As aforementioned, the energy metabolism is indispensable for the cytodifferentiation into osteoblasts. To analyze the involvement of LAL in the energy metabolism pathway during the cytodifferentiation of HPDL cells at the mRNA level, we selected the representative genes of each bioenergetic pathway, including glucose transporter 1 (*GLUT1*) for glucose uptake, lactate dehydrogenase A (*LDHA*) for glycolysis, ATP synthase F1 subunit alpha (*ATP5FA1*) for OXPHOS and carnitine palmitoyltransferase 1A (*CPT1A*) for FA oxidation. We then performed osteogenic induction without or with Lalistat-2 at a concentration of 10 μM. Then, we performed real-time PCR experiments to assess the mRNA expression levels of those metabolism-

related genes. We found that during cytodifferentiation of HPDL cells without Lalistat-2, the mRNA expression of *ATP5FA1*, *GLUT1*. and *CPT1A* was significantly up-regulated, whereas that of *LDHA* was down-regulated (Fig. 4A). These results indicated the importance of FA oxidation and OXPHOS as the major energy production pathway during the cytodifferentiation of HPDL cells. In the presence of Lalistat-2, significant downregulation of *ATP5FA1* mRNA expression was observed during cytodifferentiation of HPDL cells. However, no significant effect of Lalistat-2 was observed on the mRNA expression of *LDHA*, *GLUT1,* and *CPT1A* (Fig. 4B). These results indicated that Lalistat-2 affected OXPHOS on day 7 of the cytodifferentiation of HPDL cells; however, it did not affect glucose uptake, glycolysis pathway, and FA oxidation at the mRNA expression level. On the basis of the results at the mRNA expression level, LAL was involved in the energy metabolism of HPDL cells.

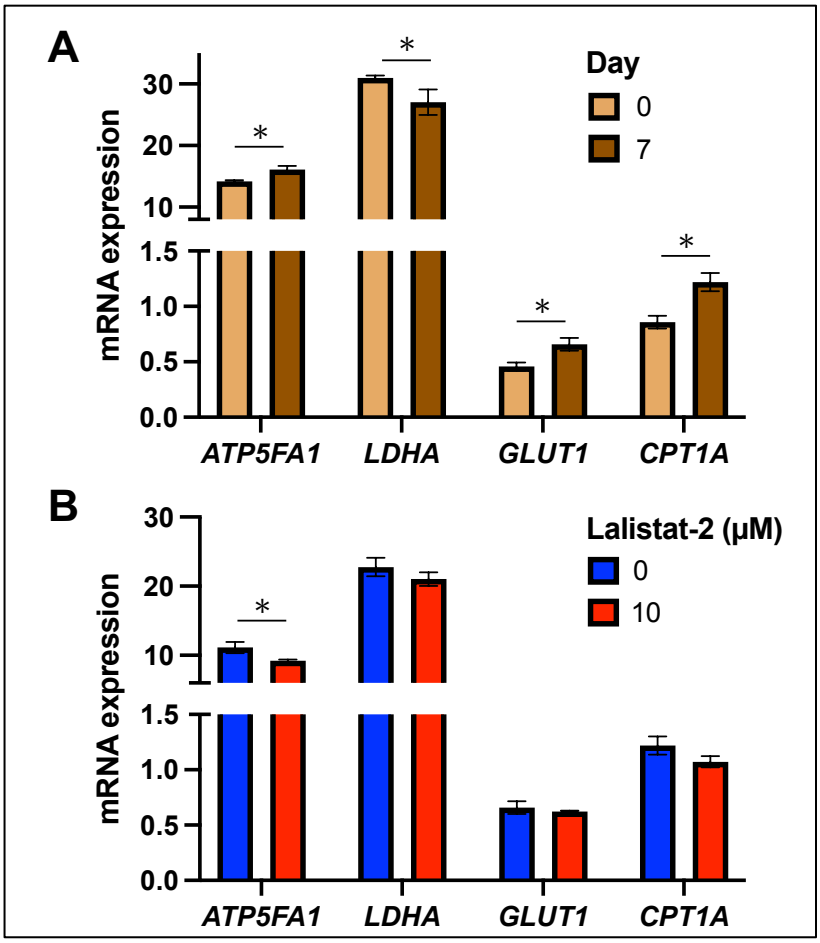

Fig. 4 LAL regulated OXPHOS-related gene expression during the cytodifferentiation of HPDL cells.

(A) HPDL cells were cultured in an osteogenic medium in the absence of Lalistat-2. The mRNA expression levels of *ATP5FA1*, *LDHA*, *GLUT1*, and *CPT1A* on day 0 and 7 of cytodifferentiation of HPDL cells were analyzed using real-time PCR. The mRNA expression of each gene was calculated as the relative ratio to that of *HPRT* (a housekeeping control gene). $^{*}p<0.05$ compared to day 0

(B) HPDL cells were cultured in an osteogenic medium without or with Lalistat-2 at a concentration of 10 μM. The mRNA expression levels of *ATP5FA1*, *LDHA*, *GLUT1*, and *CPT1A* on day 7 of the cytodifferentiation of HPDL cells were analyzed using real-time

PCR. The mRNA expression of each gene was calculated as the relative ratio to that of *HPRT*. $^{*}p<0.05$ compared to Lalistat-2 (0 μM)

(A, B) Data represent the average and SD (n=3).

4. LAL enhanced the OXPHOS pathway and supported the utilization of LDs and ATP production during cytodifferentiation of HPDL cells.

We showed that LAL affected the OXPHOS pathway at mRNA levels during cytodifferentiation. Next, we further analyzed the involvement of LAL in LD utilization and ATP production in HPDL cells during their cytodifferentiation. We first performed osteogenic induction without or with Lalistat-2 at a concentration of 10 μM. To analyze the utilization of LDs during the cytodifferentiation of HPDL cells, we stained LDs on day 0, 3, and 7 of the cytodifferentiation of HPDL cells and performed confocal microscopy. The number of LDs was reduced on day 3 and 7 of the cytodifferentiation of HPDL cells compared to those observed on day 0, indicating that LDs were utilized during the cytodifferentiation of HPDL cells (Fig. 5A). These results suggest that FAs are required for the cytodifferentiation of HPDL cells. In contrast, a high number of LDs were observed in Lalistat-2-treated HPDL cells on day 3 and 7 of the cytodifferentiation, indicating that Lalistat-2 inhibited LD utilization (Fig. 5A). These findings suggested that LAL supports the utilization of LDs for the synthesis of FAs followed by driving the OXPHOS

pathway for the cytodifferentiation of HPDL cells. Next, we measured the production rate of ATP synthesized via OXPHOS and glycolysis using the real-time ATP rate assay during the cytodifferentiation of HPDL cells with or without Lalistat-2. Without Lalistat-2, we observed a significantly increased production of ATP with OXPHOS, resulting in increased total ATP production in HPDL cells (Fig. 5B and D). This finding confirmed the importance of OXPHOS as a major energy production pathway associated with the cytodifferentiation of HPDL cells. We also observed a small but significant increase in ATP production from glycolysis on day 20 of the cytodifferentiation of HPDL cells (Fig. 5C), suggesting a possible role of glycolysis at the subsequent stage of the cytodifferentiation of HPDL cells. In contrast, Lalistat-2 significantly decreased the total ATP production rate on day 7 of the cytodifferentiation of HPDL cells, and the reduction was primarily attributed to the OXPHOS pathway (Fig. 5E). To analyze the OXPHOS-related parameters in detail, we further performed a Cell Mito Stress test to measure the basal oxygen consumption rate (OCR, an OXPHOS indicator), the baseline energetic demand of the cell, and the spare capacity, an ability of the cells to generate more ATP via the OXPHOS pathway in case of an increase in energy demand, during the cytodifferentiation of HPDL cells in the presence or absence of Lalistat-2. We found that Lalistat-2 mediated only a minor decrease in the basal OCR of HPDL cells, whereas a reduction in spare capacity was

observed (Fig. 5F and G). The result suggests that the Lalistat-2-treated HPDL cells were unable to generate additional ATP by OXPHOS during cytodifferentiation, which demands a lot of energy. Collectively, these results revealed that LAL was necessary to support the OXPHOS-dependent ATP production required during the cytodifferentiation of HPDL cells.

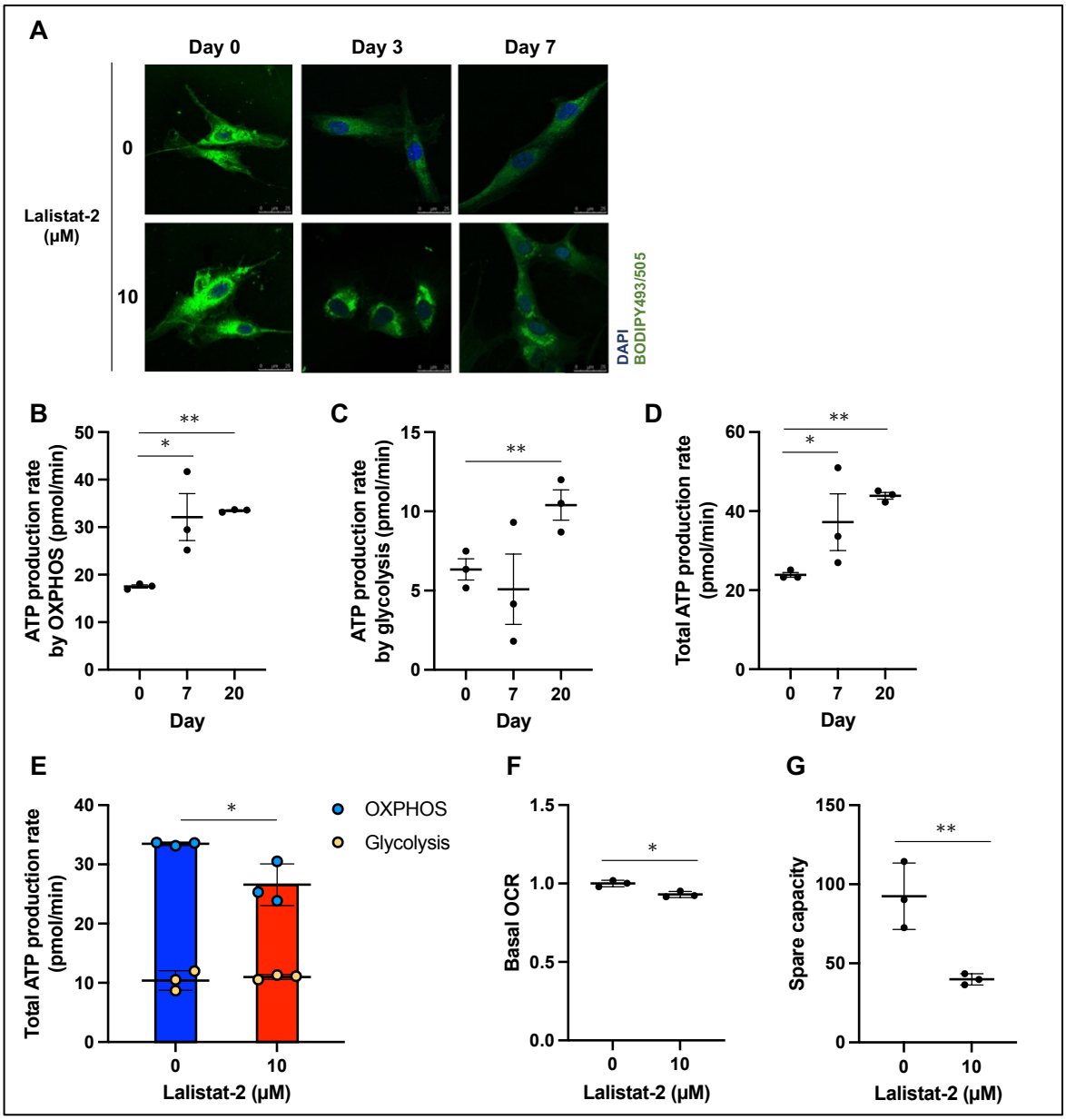

Fig. 5 LAL enhanced the OXPHOS pathway and supported the utilization of LD and ATP production during cytodifferentiation of HPDL cells.

(A) HPDL cells were cultured in an osteogenic medium without Lalistat-2. Fluorescent staining was performed to detect LDs using BODIPY493/505 on day 0, 3, and 7 of the cytodifferentiation of HPDL cells. Then, the cells were imaged by confocal microscopy. Green: LDs (BODIPY493/505) and blue: nuclei (DAPI). Scale bar: 25 μm

(B-D) The production of ATP during OXPHOS, glycolysis, and both pathways (total ATP production) on day 3, 7, and 20 of the cytodifferentiation of HPDL cells was measured using the real-time ATP rate assay. (B) ATP production rate associated with OXPHOS, (C) ATP production rate associated with glycolysis, and (D) total ATP production rate. Blue: ATP production rate associated with OXPHOS and yellow: ATP production rate associated with glycolysis. Data represent the average and SD, and dots represent each individual (n=3).

$^{*}p<0.05$, $^{**}p<0.01$ compared to day 0

(E) HPDL cells were cultured in an osteogenic medium without or with Lalistat-2 at a concentration of 10 μM. Total ATP production rate on day 7 of the cytodifferentiation of HPDL cells was measured using the real-time ATP rate assay. Data represent the average and SD, and dots represent each individual (n=3). Blue: ATP production rate associated with OXPHOS and yellow: ATP production rate associated with glycolysis.

(F-G) HPDL cells were cultured in an osteogenic medium without or with Lalistat-2 at a concentration of 10 μM. The OXPHOS-related parameters including the basal OCR (F) and the spare capacity were measured (G) on day 7 of the cytodifferentiation of HPDL cells using the Cell Mito Stress assay. The graph shows the relative ratios of the

parameters to those of untreated HPDL cells. Data represent the average and SD, and dots represent each individual (n=3).

$^{*}p<0.05$, $^{**}p<0.01$ compared to Lalistat-2 (0 μM)

Discussion

In this study, we investigated the mechanism of the regulation of the cytodifferentiation of HPDL cells by LAL regarding energy metabolism. We examined osteogenic phenotypes, mRNA expression levels of calcification- and metabolism-related genes, and metabolic phenotypes. We found that LAL is involved in the energy metabolism of HPDL cells during their cytodifferentiation by supporting required OXPHOS-dependent ATP production. Furthermore, we revealed that OXPHOS is a major pathway providing energy for HPDL cells during their cytodifferentiation. Based on our findings, we propose that LAL is important for FA production and maintains the normal conditions of OXPHOS capacity to generate adequate ATP for the cytodifferentiation of HPDL cells.

Despite limited evidence, a recent study reported that LAL is necessary for skeletal health and supports osteoblast differentiation via modulation of lipid metabolism. The negative effects on osteogenic differentiation and LD utilization were similarly observed in primary bone marrow stromal cells treated with LAL inhibitors and LAL-silenced calvarial osteoblasts. However, the effects of LAL inhibitors on mRNA expression of metabolic-related genes and metabolic phenotypes of osteoblasts have not been reported[13]. The most

recent study by Ji *et al*. showed that during the hyper-physiological condition of lipid, the LAL-dependent lipophagy was activated and restored osteoblast function of calvarial osteoblasts. In contrast, the supra-physiological condition-mediated lipophagy inhibited osteogenesis. These results emphasize the function of lipophagy in the cytodifferentiation into osteoblasts, and it implies that the effects of LAL in the cytodifferentiation are dynamic[11]. It was reported that impaired function of LAL can cause the bioenergetic alteration leading to the compromised capacity of osteoblasts during ATP-requiring activity[13]. Our finding supports this suggestion by revealing the downregulation of the OXPHOS-related gene and impaired OXPHOS capacity by Lalistat-2. The major energy production pathway used during osteoblast differentiation remains controversial. Muller *et al*. and Smith *et al*. suggested that OXPHOS is the major pathway providing energy for the cytodifferentiation of calvarial osteoblasts[27,28], whereas some studies suggested the dominant role of glycolysis during cytodifferentiation[29,30]. This discrepancy is possibly caused by differences in cell types, stage of cytodifferentiation, available substrates, cell aging, oxygen concentration, and other microenvironments. In other words, the glycolysis and OXPHOS pathways may concurrently provide energy in different proportions to maintain a balance during various stages of cytodifferentiation[21]. Our findings also support this concept as we found a significant upregulation of glycolysis-

driven ATP production at day 21 of the cytodifferentiation of HPDL cells. However, owing to the complexity of the energy metabolism, the involvement of LAL during the cytodifferentiation of HPDL cells might be affected by varied metabolic phenotypes throughout the process.

As aforementioned, osteoblast differentiation is a cellular activity that requires a large amount of ATP. Approximately 17,000 ATP equivalents are used to generate polypeptides required for collagen and matrix synthesis during hard tissue formation[6]. The tremendous need for ATP was previously believed to be generated from glucose metabolism[6,7]. However, with increasing evidence, FA oxidation has become the indispensable energy pathway required for mineralization as it can generate higher ATP[6]. Based on our results, there was an increase in total ATP production throughout the cytodifferentiation of HPDL cells. Simultaneously, we also observed the upregulation of FA-oxidation-related *CPT1A* mRNA expression and LD utilization during the cytodifferentiation of HPDL cells. Therefore, our findings emphasize the requirement of energy with the supply from FA-dependent pathways during the cytodifferentiation of HPDL cells. Likewise, Rendida-Ruedy *et al*. elucidated that intracellular LDs support osteoblast function in bone marrow stromal cells (BMSCs) by observing the impaired cytodifferentiation after treating BMSCs with Triacsin C, an inhibitor of TG

accumulation during LD formation. In addition, inhibition of CPT1 by etomoxir resulted in a decrease of OCR during the cytodifferentiation of BMSCs. While Lalistat-2 affected the cytodifferentiation of HPDL cells, it did not affect cell viability and proliferation of HPDL cells, which consume relatively lower energy. The LAL-dependent pathway may be specially required during energy-consuming activities. Although we suggest the importance of FAs as the energy substrates for energy production during the cytodifferentiation of HPDL cells, glucose and amino acids are also indispensible as we found that HPDL cells cultured in osteogenic medium with 1% FBS have reduced cytodifferentiation compared to those cultured in osteogenic medium with 10% FBS (data not shown).

Considering periodontal disease, an inflammation that deteriorates tooth-supporting apparatus, including cementum and alveolar bone, PDL cells seems to require more energy for their cytodifferentiation for regenerating and maintaining the homeostasis of periodontal tissue. LPS of periodontopathic bacteria such as *Porphyromonas gingivalis* (*Pg*) and *Actinobacillus actinomycetemcomitans* (*Aa*) is involved in onset and progression of periodontal disease[31]. Interestingly, Buechler *et al*. have reported that *Escherichia coli*-LPS downregulated the LAL expression in human blood monocytes[32], indicating the link between LPS and LAL. Similarly, we

observed the downregulation of *LIPA* mRNA expression in HPDL cells treated with *Pg*-LPS (data not shown). However, more investigations regarding the effects of LPS from different bacterial species on HPDL cells are still required to comprehend the mechanisms of LAL functions in periodontal tissue in a pathological condition.

Generally, patients with LAL deficiency experience various severe clinical symptoms, including hepatomegaly, splenomegaly, and atherosclerosis caused by the accumulation of TGs and CEs[33]. Besides AgP-associated *LIPA* SNP rs143793106 which we had previously reported[22], the other SNPs of *LIPA* rs1412444 and rs2246833 have been also identified as genetic risk factors for coronary heart disease[34]. Additionally, impaired function of LAL is involved in non-alcoholic fatty liver disease (NAFLD)[35]. Although the mechanisms have not been elucidated, increasing evidence suggests associations between periodontal disease and systemic diseases, including coronary heart disease[36], NAFLD[37], obesity[38], and atherosclerosis[39]. Therefore, LAL-related energy metabolism can bridge the gap and enhance to understand their relationships.

The specific microenvironments, including oxygen availability and micronutrients, affect the metabolic programming of the cells. The altered

microenvironment was also observed in the subgingival periodontal pocket under periodontitis. Multiple studies have reported hypoxia, a condition with less oxygen supply, and altered bacterial species with an increase in pocket depth[40-42]. Hypoxia reportedly affects the PDL cells during homeostasis and cytodifferentiation. Li *et al*. have revealed by proteomic analysis that hypoxic condition was associated with the pathways of energy metabolism, autophagy, and responses to the stimuli in HPDL cells[43]. Xiao *et al*. found that hypoxia suppresses the proliferation and migration of HPDL cells[44]. However, the effects of hypoxic conditions on cytodifferentiation are still controversial. Osathanon *et al*. have reported reduced ALPase activity and calcification-related genes in hypoxia-stimulating cobalt chloride-treated HPDL cells during their cytodifferentiation[45]. In contrast, Li *et al*. reported the upregulation of calcification-related genes in hypoxia-mimicking dimethyloxalylglycine-treated HPDL cells[46]. Mimicking the *in vivo* hypoxic condition by *in vitro* experiments is challenging. However, the alteration of oxygen availability can clearly lead to a metabolic shift inside the cells. Generally, oxygen deprivation upregulates the expression of hypoxia-inducible factor 1 (HIF-1), leading to the shift from oxygen-driven OXPHOS to glycolysis. Ng *et al*. have observed a significant increase in the proportion of *HIF1A*-expressing fibroblast-like cells from the gingival biopsy[47]. The protein level of HIF1α in the diseased periodontal pockets was also higher than that in the control gingival samples[47].

Similarly, Noguchi *et al*. have detected that *HIF1B* mRNA expression in the gingival samples with a sulcular depth of 2 to 4 mm was higher than that with a sulcular depth of less than 2 mm[48]. Owing to the influence of HIF-1, glycolysis is possibly more preferred for the energy production in the oxygen-deprived deep periodontal pockets than that in the shallow sites. Furthermore, Takedachi *et al*. have recently reported that HIF-1 is negatively regulated by periodontal ligament-associated protein-1 (PLAP-1), a preferentially expressed protein in HPDL cells, under hypoxic condition. They suggested the roles of PLAL-1 in PDL by regulating hypoxic responses[49]. However, the mechanism was not fully elucidated. Interestingly, we also found that LAL inhibition by Lalistat-2 altered *HIF1A* mRNA expression during the HPDL-cell cytodifferentiation (data not shown). LAL, as well as energy metabolism, might involve the regulation of responses to hypoxia and PLAL-1 functions in HPDL cells.

In addition to oxygen, glucose plays an important role in the metabolic phenotype and affects the osteoblastic differentiation of HPDL cells. Glucose deprivation results in reduced ATP production. However, the effects of HG on osteoblast differentiation are still controversial and inconclusive. For example, Suebbuk *et al*. have observed that HG enhances the cytodifferentiation of HPDL fibroblasts[17]. On the contrary, Zhen *et al*. have reported the suppression

of the cytodifferentiation of HPDL stem cells by HG[19]. In our study, we performed the osteogenic induction using a growth medium containing approximately 100–110 mg/dL, which is in the normal range of healthy non-fasting blood glucose levels[50]. This concentration of glucose is also used by *in vivo* experiments as the approximate glucose concentration at 100 mg/dL in laboratory mice fed with a normal diet[51-53].

In our study, we have 3 limitations. First, as previously mentioned, any changes in oxygen and glucose availability can cause metabolic alteration. To avoid the influences of oxygen and glucose on the cytodifferentiation of HPDL cells, we performed the experiments in a single setting: oxygen concentration (21%) and glucose concentration (100–110 mg/dL). Further studies with various environmental settings will provide us with more information of LAL functions during the cytodifferentiation of HPDL cells in closer to *in vivo* conditions. Second, our findings were obtained from *in vitro* experiments. The future *in vivo* experiments are warranted to evaluate the regeneration of the alveolar bone volume and the preference of energy metabolism pathway in PDL tissue under the recovery from periodontitis in LAL knock-out mice. Last, we analyzed the metabolic phenotypes of only major pathways, OXPHOS, and glycolysis. The effects of LAL on the phenotypes of the sub-

metabolic pathways, such as FA and amino acid oxidation, should be analyzed in the future.

Currently, an enzyme replacement therapy using sabelipase alfa, a recombinant LAL, is approved for the effective treatment of LAL deficiency[54,55]. In addition, peroxisome proliferator-activated receptor alpha (PPAR-α) agonist has been reported to rescue impaired function of LAL by enhancing LAL expression in HepG2 cells, a cell line of human liver carcinoma cells[35]. These molecules might affect the cytodifferentiation of HPDL cells with impaired LAL function as well. Furthermore, Gomaraschi *et al*. have mentioned that LAL supplies FAs to support immune cell functions, and that restoring LAL activity improves metabolic parameters and mitigates the immunoinflammatory response. They have proposed that targeting LAL may be a therapeutic strategy to recover the impaired functions of immune cells[35]. As we have proposed the energy metabolism of PDL cells for future periodontal regeneration, we strongly believe that targeting LAL-related energy metabolism will be a novel strategy for periodontal treatment[21].

Conclusion

In this study, we revealed the followings:

1. Lalistat-2 inhibited LAL activity and LD utilization in HPDL cells, but not viability and proliferation of HPDL cells.
2. *LIPA* gene expression was upregulated during the cytodifferentiation of HPDL cells.
3. Inhibition of LAL by Lalistat-2 suppressed the cytodifferentiation of HPDL cells.
4. LAL was involved in the energy metabolism during the cytodifferentiation of HPDL cells. Particularly, LAL regulated the OXPHOS-related gene, *ATP5FA1*, during the cytodifferentiation of HPDL cells.
5. LAL enhanced the OXPHOS pathway and supported LD utilization and ATP production during the cytodifferentiation of HPDL cells. In contrast, the inhibition of LAL by Lalistat-2 decreased ATP production from OXPHOS and the spare capacity of OCR.

These results suggest that LAL utilizes LDs to drive the OXPHOS pathway, resulting in adequate ATP production to support the proper cytodifferentiation of HPDL cells and maintain the homeostasis of periodontal

tissue. In contrast, in a pathological condition such as periodontitis, it is suggested that LPS produced by periodontal pathogens impairs LAL functions, resulting in disturbing LD utilization and ATP production from OXPHOS. As a result, HPDL cells could not meet the energy demand for their cytodifferentiation, leading to the destruction of alveolar bone (Fig. 6).

On the basis of these findings, we elucidated a possible mechanism of which LAL regulates the pathophysiological conditions of periodontal tissue through energy metabolism.

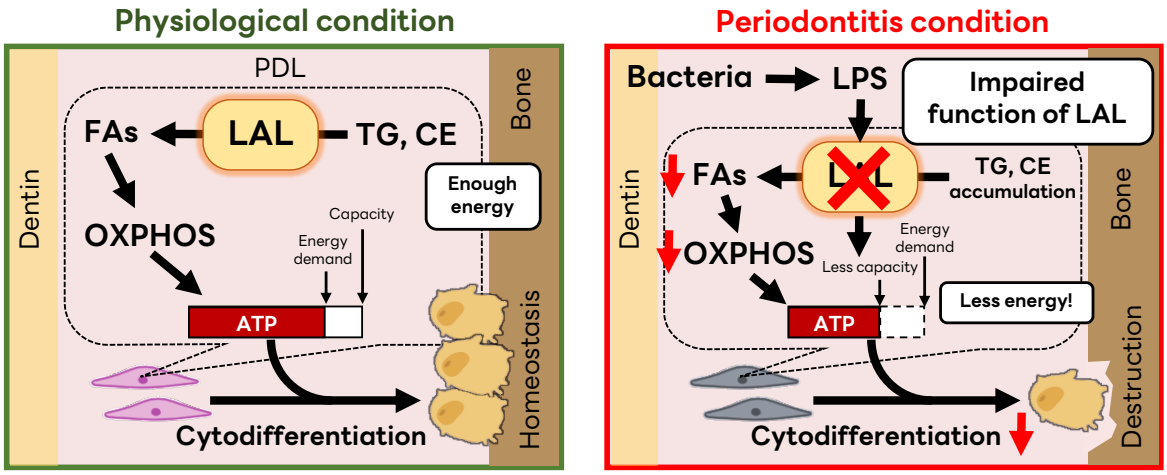

Fig. 6 A possible mechanism of which LAL regulates the pathophysiological conditions of periodontal tissue through energy metabolism.

Left: During a physiological condition, LAL hydrolyzes triglycerides (TGs) and cholesteryl esters (CEs) to generate fatty acids (FAs). FAs are further supplied to the oxidative phosphorylation (OXPHOS) pathway to generate adequate ATP demanded during the cytodifferentiation of HPDL cells to maintain periodontal tissue homeostasis. *Right*: Under periodontitis condition, lipopolysaccharides (LPS), produced from periodontopathic bacteria, impairs LAL function resulting in reduced FAs supplying the OXPHOS pathway, and impaired OXPHOS capacity. HPDL cells cannot generate adequate ATP to reach the demand during their cytodifferentiation, leading to the destruction of bone.

ATP: adenosine triphosphate, PDL: periodontal ligament

Acknowledgment

The author got substantial support and assistance during completing the Ph.D. study and writing the dissertation.

First and foremost, I wish to express my heartfelt gratitude to Professor Murakami Shinya, my dissertation supervisor, for his invaluable advice and vast expertise. I also express gratitude to him for providing me with the opportunity to study at Osaka University, Japan.

I would like to express my heartfelt gratitude to Assistant Professor Fujihara Chiharu, my dissertation co-supervisor, who assisted me in every detail of my studies and life in Osaka with her intelligence, skills, and unmatched kindness.

Grateful acknowledgment is given to the Government of Thailand and Srinakharinwirot University, my donor, for giving me the fund and opportunity to study at Osaka University.

My sincere thanks go to the Laboratory of Immunosenescence, National Institutes of Biomedical Innovation, Health and Nutrition for providing me with the extracellular flux analyzer and additional support for my experiments.

Additionally, I'd like to thank all the members of the Department of Periodontology for their support of my work and personal life, as well as my family and friends for their encouragement throughout the years of study.

References

1. Dunn J, Grider MH. Physiology, Adenosine Triphosphate. [Updated 2022 Feb 17]. In. *StatPearls [Internet]*. Treasure Island (FL): StatPearls Publishing; 2022 Jan-. Available from: https://www.ncbi.nlm.nih.gov/books/NBK553175/.
2. Yao CH, Wang R, Wang Y, Kung CP, Weber JD, Patti GJ. Mitochondrial fusion supports increased oxidative phosphorylation during cell proliferation. *Elife.* 2019;8:e41351.
3. Shin B, Benavides GA, Geng J, et al. Mitochondrial Oxidative Phosphorylation Regulates the Fate Decision between Pathogenic Th17 and Regulatory T Cells. *Cell Rep.* 2020;30(6):1898-1909 e1894.
4. Desousa BR, Kim KKO, Hsieh WY, et al. Calculating ATP production rates from oxidative phosphorylation and glycolysis during cell activation. *bioRxiv.* 2022:2022.2004.2016.488523.
5. Lee WC, Ji X, Nissim I, Long F. Malic Enzyme Couples Mitochondria with Aerobic Glycolysis in Osteoblasts. *Cell Rep.* 2020;32(10):108108.
6. Kushwaha P, Wolfgang MJ, Riddle RC. Fatty acid metabolism by the osteoblast. *Bone.* 2018;115:8-14.

7. Donat A, Knapstein PR, Jiang S, et al. Glucose Metabolism in Osteoblasts in Healthy and Pathophysiological Conditions. *Int J Mol Sci.* 2021;22(8):4120.

8. Da Poian A, BACHA T, Luz M. Nutrient utilization in humans: metabolic pathways. *Nature Education.* 2010;3(9):11.

9. Pirahanchi Y, Sharma S. Biochemistry, Lipase. [Updated 2022 Jul 11]. In. *StatPearls [Internet]*. Treasure Island (FL): StatPearls Publishing; 2022 Jan-. Available from: https://www.ncbi.nlm.nih.gov/books/NBK537346/.

10. Winkler FK, D'Arcy A, Hunziker W. Structure of human pancreatic lipase. *Nature.* 1990;343(6260):771-774.

11. Ji C, Zhang Z, Xu X, Song D, Zhang D. Hyperlipidemia impacts osteogenesis via lipophagy. *Bone.* 2023;167:116643.

12. Li F, Zhang H. Lysosomal Acid Lipase in Lipid Metabolism and Beyond. *Arterioscler Thromb Vasc Biol.* 2019;39(5):850-856.

13. Helderman RC, Whitney DG, Duta-Mare M, et al. Loss of function of lysosomal acid lipase (LAL) profoundly impacts osteoblastogenesis and increases fracture risk in humans. *Bone.* 2021;148:115946.

14. Beertsen W, McCulloch CA, Sodek J. The periodontal ligament: a unique, multifunctional connective tissue. *Periodontol 2000.* 1997;13:20-40.

15. McCulloch CA. Origins and functions of cells essential for periodontal repair: the role of fibroblasts in tissue homeostasis. *Oral Dis.* 1995;1(4):271-278.

16. Li J, Wang Z, Huang X, et al. Dynamic proteomic profiling of human periodontal ligament stem cells during osteogenic differentiation. *Stem Cell Res Ther.* 2021;12(1):98.

17. Seubbuk S, Sritanaudomchai H, Kasetsuwan J, Surarit R. High glucose promotes the osteogenic differentiation capability of human periodontal ligament fibroblasts. *Mol Med Rep.* 2017;15(5):2788-2794.

18. Liu Z, Chen T, Sun W, et al. DNA Demethylation Rescues the Impaired Osteogenic Differentiation Ability of Human Periodontal Ligament Stem Cells in High Glucose. *Sci Rep.* 2016;6:27447.

19. Zhen L, Jiang X, Chen Y, Fan D. MiR-31 is involved in the high glucose-suppressed osteogenic differentiation of human periodontal ligament stem cells by targeting Satb2. *Am J Transl Res.* 2017;9(5):2384-2393.

20. Symmank J, Chorus M, Appel S, et al. Distinguish fatty acids impact survival, differentiation and cellular function of periodontal ligament fibroblasts. *Sci Rep.* 2020;10(1):15706.

21. Fujihara C, Nantakeeratipat T, Murakami S. Energy Metabolism in Osteogenic Differentiation and Reprogramming: A Possible Future

Strategy for Periodontal Regeneration. *Frontiers in Dental Medicine.* 2022;3:815140.

22. Matsumoto M, Fujihara C, Nantakeeratipat T, et al. Lipase-a single-nucleotide polymorphism rs143793106 is associated with increased risk of aggressive periodontitis by negative influence on the cytodifferentiation of human periodontal ligament cells. *J Periodontal Res.* 2022:175-183.

23. Kitagaki J, Miyauchi S, Asano Y, et al. A Putative Association of a Single Nucleotide Polymorphism in GPR126 with Aggressive Periodontitis in a Japanese Population. *PLoS One.* 2016;11(8):e0160765.

24. Kitagaki J, Miyauchi S, Xie CJ, et al. Effects of the proteasome inhibitor, bortezomib, on cytodifferentiation and mineralization of periodontal ligament cells. *J Periodontal Res.* 2015;50(2):248-255.

25. Bessey OA, Lowry OH, Brock MJ. A method for the rapid determination of alkaline phosphates with five cubic millimeters of serum. *J Biol Chem.* 1946;164:321-329.

26. Dahl LK. A simple and sensitive histochemical method for calcium. *Proc Soc Exp Biol Med.* 1952;80(3):474-479.

27. Muller DIH, Stoll C, Palumbo-Zerr K, et al. PPARdelta-mediated mitochondrial rewiring of osteoblasts determines bone mass. *Sci Rep.* 2020;10(1):8428.

28. Smith CO, Eliseev RA. Energy Metabolism During Osteogenic Differentiation: The Role of Akt. *Stem Cells Dev.* 2021;30(3):149-162.

29. Hong M, Zhang XB, Xiang F, Fei X, Ouyang XL, Peng XC. MiR-34a suppresses osteoblast differentiation through glycolysis inhibition by targeting lactate dehydrogenase-A (LDHA). *In Vitro Cell Dev Biol Anim.* 2020;56(6):480-487.

30. Wu Y, Wang M, Feng H, et al. Lactate induces osteoblast differentiation by stabilization of HIF1alpha. *Mol Cell Endocrinol.* 2017;452:84-92.

31. Socransky SS, Haffajee AD. The bacterial etiology of destructive periodontal disease: current concepts. *J Periodontol.* 1992;63(4 Suppl):322-331.

32. Buechler C, Ullrich H, Aslanidis C, et al. Lipoprotein (a) downregulates lysosomal acid lipase and induces interleukin-6 in human blood monocytes. *Biochim Biophys Acta.* 2003;1642(1-2):25-31.

33. Burton BK, Deegan PB, Enns GM, et al. Clinical Features of Lysosomal Acid Lipase Deficiency. *J Pediatr Gastroenterol Nutr.* 2015;61(6):619-625.

34. Wild PS, Zeller T, Schillert A, et al. A genome-wide association study identifies LIPA as a susceptibility gene for coronary artery disease. *Circ Cardiovasc Genet.* 2011;4(4):403-412.

35. Gomaraschi M, Fracanzani AL, Dongiovanni P, et al. Lipid accumulation impairs lysosomal acid lipase activity in hepatocytes: Evidence in NAFLD patients and cell cultures. *Biochim Biophys Acta Mol Cell Biol Lipids.* 2019;1864(12):158523.

36. Humphrey LL, Fu R, Buckley DI, Freeman M, Helfand M. Periodontal disease and coronary heart disease incidence: a systematic review and meta-analysis. *J Gen Intern Med.* 2008;23(12):2079-2086.

37. Kuraji R, Sekino S, Kapila Y, Numabe Y. Periodontal disease-related nonalcoholic fatty liver disease and nonalcoholic steatohepatitis: An emerging concept of oral-liver axis. *Periodontol 2000.* 2021;87(1):204-240.

38. Martinez-Herrera M, Silvestre-Rangil J, Silvestre FJ. Association between obesity and periodontal disease. A systematic review of epidemiological studies and controlled clinical trials. *Med Oral Patol Oral Cir Bucal.* 2017;22(6):e708-e715.

39. Zardawi F, Gul S, Abdulkareem A, Sha A, Yates J. Association Between Periodontal Disease and Atherosclerotic Cardiovascular Diseases: Revisited. *Front Cardiovasc Med.* 2020;7:625579.

40. Loesche WJ, Gusberti F, Mettraux G, Higgins T, Syed S. Relationship between oxygen tension and subgingival bacterial flora in untreated human periodontal pockets. *Infect Immun.* 1983;42(2):659-667.

41. Mettraux GR, Gusberti FA, Graf H. Oxygen tension (pO2) in untreated human periodontal pockets. *J Periodontol.* 1984;55(9):516-521.

42. Shi M, Wei Y, Hu W, Nie Y, Wu X, Lu R. The Subgingival Microbiome of Periodontal Pockets With Different Probing Depths in Chronic and Aggressive Periodontitis: A Pilot Study. *Front Cell Infect Microbiol.* 2018;8:124.

43. Li Q, Luo T, Lu W, Yi X, Zhao Z, Liu J. Proteomic analysis of human periodontal ligament cells under hypoxia. *Proteome Sci.* 2019;17:3.

44. Xiao Z, Han Y, Zhang Y, Zhang X. Hypoxia-regulated human periodontal ligament cells via Wnt/beta-catenin signaling pathway. *Medicine (Baltimore).* 2017;96(16):e6562.

45. Osathanon T, Vivatbutsiri P, Sukarawan W, Sriarj W, Pavasant P, Sooampon S. Cobalt chloride supplementation induces stem-cell marker expression and inhibits osteoblastic differentiation in human periodontal ligament cells. *Arch Oral Biol.* 2015;60(1):29-36.

46. Li S, Shao J, Zhou Y, et al. The impact of Wnt signalling and hypoxia on osteogenic and cementogenic differentiation in human periodontal ligament cells. *Mol Med Rep.* 2016;14(6):4975-4982.

47. Ng KT, Li JP, Ng KM, Tipoe GL, Leung WK, Fung ML. Expression of hypoxia-inducible factor-1alpha in human periodontal tissue. *J Periodontol.* 2011;82(1):136-141.

48. Noguchi K, Miwa Y, Sunohara M, Sato I. Analysis of vascular distribution and growth factors in human gingival tissue associated with periodontal probing depth. *Okajimas Folia Anat Jpn.* 2011;88(2):75-83.

49. Takedachi M, Yamamoto S, Kawasaki K, et al. Reciprocal role of PLAP-1 in HIF-1alpha-mediated responses to hypoxia. *J Periodontal Res.* 2022;57(3):470-478.

50. Moebus S, Gores L, Losch C, Jockel KH. Impact of time since last caloric intake on blood glucose levels. *Eur J Epidemiol.* 2011;26(9):719-728.

51. Attane C, Peyot ML, Lussier R, et al. Differential Insulin Secretion of High-Fat Diet-Fed C57BL/6NN and C57BL/6NJ Mice: Implications of Mixed Genetic Background in Metabolic Studies. *PLoS One.* 2016;11(7):e0159165.

52. Paul DS, Walton FS, Saunders RJ, Styblo M. Characterization of the impaired glucose homeostasis produced in C57BL/6 mice by chronic exposure to arsenic and high-fat diet. *Environ Health Perspect.* 2011;119(8):1104-1109.

53. Sun C, Xinzhi L, Liu L, et al. Effect of fasting time on measuring mouse blood glucose level. 2016;9:4186-4189.

54. Frampton JE. Sebelipase Alfa: A Review in Lysosomal Acid Lipase Deficiency. *Am J Cardiovasc Drugs.* 2016;16(6):461-468.

55. Pastores GM, Hughes DA. Lysosomal Acid Lipase Deficiency: Therapeutic Options. *Drug Des Devel Ther.* 2020;14:591-601.